

Molecular Physics

An International Journal at the Interface Between Chemistry and Physics

ISSN: (Print) (Online) Journal homepage: <https://www.tandfonline.com/loi/tmph20>

Generalized Sturmian Functions in prolate spheroidal coordinates

D. M. Mitnik , F. A. López & L. U. Ancarani

To cite this article: D. M. Mitnik , F. A. López & L. U. Ancarani (2021): Generalized Sturmian Functions in prolate spheroidal coordinates, Molecular Physics, DOI: [10.1080/00268976.2021.1881179](https://doi.org/10.1080/00268976.2021.1881179)

To link to this article: <https://doi.org/10.1080/00268976.2021.1881179>



Published online: 08 Feb 2021.



Submit your article to this journal [↗](#)



Article views: 6



View related articles [↗](#)



View Crossmark data [↗](#)

Generalized Sturmian Functions in prolate spheroidal coordinates

D. M. Mitnik^a, F. A. López^a and L. U. Ancarani^b

^aInstituto de Astronomía y Física del Espacio (IAFE), CONICET-UBA, Buenos Aires, Argentina; ^bUniversité de Lorraine, CNRS, LPCT, Metz, France

ABSTRACT

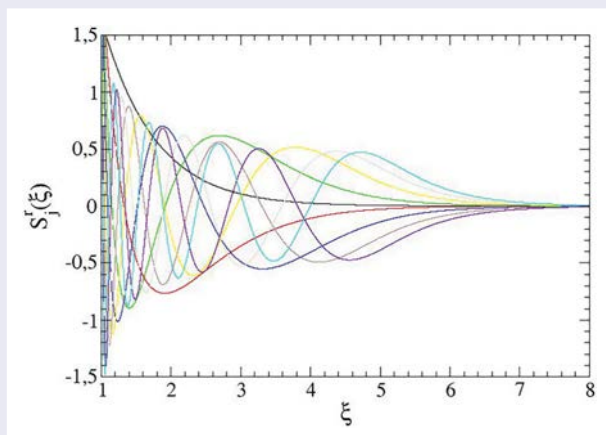
With the aim of describing bound and continuum states for diatomic molecules, we develop and implement a spectral method that makes use of Generalized Sturmian Functions (GSF) in prolate spheroidal coordinates. In order to master all computational issues, we apply it here to one-electron molecular ions and compare with benchmark data for both ground and excited states. We actually propose two different schemes to solve the two coupled differential equations. The first one is an iterative 1*d* procedure in which one solves alternately the angular and the radial equations, the latter yielding the state energy. The second, named direct 2*d* method, consists in representing the Hamiltonian matrix in a two-dimensional GSF basis set, and its further diagonalization. Both spectral schemes are timewise computationally efficient and very accurate results are obtained with minimal basis sets. This is related on one side to the use of the natural coordinate system and, on the other, to the intrinsic good property of all GSF basis elements that are constructed as to obey appropriate physical boundary conditions. The present implementation for bound states paves the way for the study of continuum states involved in ionization of one or two-electron diatomic targets.

ARTICLE HISTORY

Received 6 July 2020
Accepted 3 December 2020

KEYWORDS

Diatomic molecules; prolate spheroidal coordinates; spectral methods; Generalized Sturmian Functions



1. Introduction

The molecular ion H_2^+ , as well as the isotopic forms such as HD^+ or D_2^+ , and other one-electron diatomics such as HHe^{+2} or HLi^{+3} , are the simplest molecular quantum three-body problem with Coulomb interactions. H_2^+ , in particular, has been largely studied since the early days of quantum mechanics [1–3], and is presented in standard molecular physics books as it allows one to understand why molecules form. On top of being important in astrophysics (it is involved in many reaction chains leading to the production of polyatomic molecules), the

molecular ion H_2^+ also serves as a benchmark to test any new molecular approach and numerical method.

In the fixed-nuclei approximation, it is well known that prolate spheroidal coordinates make the Schrödinger equation separable [4]. Aside from the simple azimuthal angle dependence due to axial symmetry, the wavefunction depends on two variables, one angular and one radial (actually quasi-angular and quasi-radial). The H_2^+ bound structure can be found by solving a system of two coupled ordinary differential equations, one for each of these two variables. An analytical solution exists formally [1–3] but

involves two not so tractable expansions and therefrom complicated energy equations (see, e.g. [5] and references therein). In practice, therefore, the energies are found numerically. This is why a wide variety of methods, including iterative methods, have been proposed and applied to solve the coupled equations. For continuum states, necessary for example to describe ionisation processes from diatomic molecules, the energy is known and fixed. However, these non- L^2 states are much more difficult to build as they oscillate up to infinity. Some recent investigations dedicated to their description in prolate spheroidal coordinates include [6,7]. Approximate single or double continuum wavefunctions borrowed from the atomic literature have been extended to the two-centre case and employed to study ionisation processes [8–11]. Other approaches consist in extending well established atomic numerical techniques to the diatomic molecular case, using (see, e.g. [12,13]) or not using (see, e.g. [14]) prolate spheroidal coordinates.

In the last decade, a spectral method named GSF has been developed and implemented to study the structure of and scattering processes on atomic systems [15,16]. The method uses complete and orthogonal basis sets of Generalized Sturmian Functions (GSF) with appropriate boundary conditions. Negative energy GSFs allow one to study bound states. The helium atom, the simplest atomic quantum three-body problem with Coulomb interactions, served as a benchmark to put the method on solid grounds, by studying in details convergence issues, the integrals involved and the adequate choice of optimal parameters and numerical packages (see [17] and references therein). While the aim of the GSF method was not to compete with well-established structure codes, it proved to be very accurate at a reduced computational cost because of intrinsic GSF properties, in particular, the adequate, and unique, asymptotic decay of all basis elements.

After bound states, the GSF approach was rapidly implemented for continuum states for which the good properties of positive energy GSFs demonstrated the power of the method. Indeed, for continuum states, the correct asymptotic behaviour is crucial in any scattering calculation as shown in applications to one and two-electron atomic systems (see, e.g. [18–20]). The method was first presented in spherical coordinates, then extended to hyperspherical coordinates but limited to atomic systems. An extension to molecules with a heavy central nucleus has been proposed in a one-centre GSF approach [21] and applied to ionisation processes [22–24]. Nothing, however, has been proposed to deal with diatomic molecules.

The purpose of this manuscript is to develop and implement a GSF method in prolate spheroidal coordinates, thus combining the two advantages of (i) using the natural coordinates for diatomic systems and (ii) the power of a spectral method together with the intrinsically good GSF properties. The long term aim is to be able to describe accurately single or double ionisation of diatomic molecules treated as a two-electron system. The development will follow a path similar to the one adopted for the atomic case. We will first consider bound one-electron molecules before moving to the continuum part of the spectrum. By studying benchmark one-electron molecular ions, such as the H_2^+ , we wish to validate the new computational procedure and code, check thoroughly all convergence and precision issues, and test the robustness with respect to the variation of the internuclear distance.

We actually present here two distinct computational methods that serve different purposes. In the first one, we adopt an iterative approach, solving alternately the separated Schrödinger equations for the angular part and for the radial part. This iterative $1d$ procedure, which is repeated until convergence, presents the novelty of using GSF with appropriate boundary conditions. Because of such property, the approach results to be computationally efficient as only small basis are needed to obtain very good energy levels. It is also efficient in computing time because the GSF basis elements already solve the Hamiltonian differential operator so that no derivative calculation is needed at each iteration. The present study allows us to establish the capability of the approach and master the related parameters when using appropriate GSF in prolate spheroidal coordinates. The iterative $1d$ procedure puts the focus on the energy and wave function of a single molecular state. The second method, called here the direct $2d$ method, has a different scope since it provides a set of states at the same time. It consists in representing the Hamiltonian matrix in a two-dimensional GSF basis set, and its further diagonalisation. On top of the same advantages as the first method, the $2d$ spectral approach demonstrates its full power by providing accurately many states simultaneously, and this with very small basis.

The remainder of this paper is as follows. In Section 2, we provide the theoretical framework of the proposed GSF method in prolate spheroidal coordinates. Then, in Section 3, we apply it to the ground and first three excited states of symmetric (H_2^+) and asymmetric (HHe^{+2} and HLi^{+3}) molecular ions. The successful comparison with benchmark data from the literature allows us to validate the method for bound states. As indicated in the Conclusion (Section 5), the next step will be to study continuum

states for which positive energy GSF, with appropriate boundary conditions, will be used.

Atomic units ($\hbar = m_e = e = 1$) are assumed throughout.

2. Theory

Consider a diatomic molecular system consisting of one electron and two nuclei of arbitrary charges Z_1 and Z_2 placed at a fixed distance R along a line defining the z axis; let r_1 denote the distance of the electron from nucleus 1 and r_2 from nucleus 2. To simplify, we neglect any nuclei finite mass effect.

In prolate spheroidal coordinates, defined by

$$\xi \equiv \frac{r_1 + r_2}{R}; \quad \eta \equiv \frac{r_1 - r_2}{R}; \quad \phi \equiv \arctan\left(\frac{y}{x}\right), \quad (1)$$

where $1 \leq \xi < \infty$, $-1 \leq \eta \leq 1$ and $0 \leq \phi \leq 2\pi$, the Schrödinger equation for the electron reads

$$\left\{ -\frac{2}{R^2(\xi^2 - \eta^2)} \left[\frac{\partial}{\partial \xi} (\xi^2 - 1) \frac{\partial}{\partial \xi} + \frac{\partial}{\partial \eta} (1 - \eta^2) \frac{\partial}{\partial \eta} + \frac{\xi^2 - \eta^2}{(\xi^2 - 1)(1 - \eta^2)} \frac{\partial^2}{\partial \phi^2} \right] + V(\eta, \xi) \right\} \psi(\xi, \eta, \phi) = E\psi(\xi, \eta, \phi), \quad (2)$$

with the electron-nuclei potential given by

$$V(\xi, \eta) = -\frac{Z_1}{r_1} - \frac{Z_2}{r_2} = -\frac{2}{R} \frac{(Z_1 + Z_2)\xi - (Z_1 - Z_2)\eta}{(\xi^2 - \eta^2)}. \quad (3)$$

In the fixed-nuclei approximation, the internuclear distance R enters as a parameter, and the nuclei repulsive potential energy $1/R$ may be simply added. Equation (2) is separable in these coordinates, meaning that the solution is expressed as a product of three functions

$$\psi(\xi, \eta, \phi) = U(\xi)\Lambda(\eta)\Phi(\phi). \quad (4)$$

The azimuthal function Φ is easily separated, and must fulfill the equation

$$\frac{d^2\Phi}{d\phi^2} + m^2\Phi = 0, \quad (5)$$

whose solutions are

$$\Phi(\phi) = \frac{1}{\sqrt{2\pi}} e^{im\phi}, \quad (6)$$

with $m = 0, \pm 1, \pm 2, \pm 3, \dots$. Because of the axial symmetry of the potential, m is a good quantum number.

Upon elimination of the azimuthal dependence, and defining $p^2 = -\frac{R^2 E}{2}$, $a_1 = R(Z_1 - Z_2)$ and $a_2 = R(Z_1 +$

$Z_2)$, the ensuing equation reads

$$\left\{ \frac{\partial}{\partial \xi} \left[(\xi^2 - 1) \frac{\partial}{\partial \xi} \right] + a_2 \xi - p^2 \xi^2 - \frac{m^2}{\xi^2 - 1} + \frac{\partial}{\partial \eta} \left[(1 - \eta^2) \frac{\partial}{\partial \eta} \right] - a_1 \eta + p^2 \eta^2 - \frac{m^2}{1 - \eta^2} \right\} U(\xi)\Lambda(\eta) = 0 \quad (7)$$

and is also separable. Denoting the separation constant as A , one obtains a system of two non-trivial ordinary differential equations, a ‘radial’ equation for $U(\xi)$ and an ‘angular’ equation for $\Lambda(\eta)$,

$$\left[\frac{\partial}{\partial \xi} \left[(\xi^2 - 1) \frac{\partial}{\partial \xi} \right] + a_2 \xi - p^2 \xi^2 - \frac{m^2}{\xi^2 - 1} + A \right] U(\xi) = 0, \quad (8a)$$

$$\left[\frac{\partial}{\partial \eta} \left[(1 - \eta^2) \frac{\partial}{\partial \eta} \right] - a_1 \eta + p^2 \eta^2 - \frac{m^2}{1 - \eta^2} - A \right] \Lambda(\eta) = 0, \quad (8b)$$

which are coupled through both the scaled energy p and the coupling constant A . States with different m values are not coupled, so that they can be considered independently.

In this work, we propose two different methods using a spectral approach based on GSF in prolate spheroidal coordinates. In the first – named hereafter ‘iterative 1d method’ – we solve, alternately, the one-dimensional radial equation (8a), assuming a given separation constant A , and solving an eigenvalue equation for the scaled energy p . Then, we use this energy as a fixed value in the one-dimensional angular equation (8b), obtaining a new separation constant A . The process is repeated until convergence is achieved. In this iterative procedure, both equations are solved by using adequate GSF basis sets and are converted into eigenvalue problems. The main advantage of our GSF approach resides in the fact that the principal part of these two equations (in particular, the derivatives) are already dealt with by the basis functions; as a consequence, derivative calculations are not required at every iteration step. In the second method, we construct a basis set composed of products of the angular and radial GSF. This two-dimensional basis is used to represent the Hamiltonian, which is diagonalised in order to solve the whole Schrödinger equation (2). In this way, we obtain the eigenvalues (energies) and eigenvectors (solutions) of many states at the same time. This method, here referred to as the ‘direct 2d method’, while possessing the same advantages related to GSF is computationally even more efficient.

2.1. GSF: iterative 1d method

2.1.1. Angular equation

We search the solution of Equation (8b), for a given m , as an expansion in Sturmian functions

$$\Lambda(\eta) = \sum_j c_j S_j^a(\eta), \quad (9)$$

the angular basis set being generated by solving the Sturmian equation

$$\left[\frac{\partial}{\partial \eta} \left[(1 - \eta^2) \frac{\partial}{\partial \eta} \right] - \frac{m^2}{1 - \eta^2} \right] S_j^a(\eta) = -\beta_j S_j^a(\eta), \quad (10)$$

with boundary conditions $S_j^a(1) = 1$ and $S_j^a(-1) = (-1)^j$ for $m = 0$ and $S_j^a(1) = S_j^a(-1) = 0$ for $m \neq 0$. The solutions are actually the well-known associated Legendre polynomials [25], $S_j^a(\eta) = P_j^m(\eta)$, and correspond to eigenvalues $\beta_j = j(j+1)$. Figure 1 shows the first 9 elements $S_j^a(\eta)$ for $m = 0$.

With expansion (9) and making use of Equation (10), the angular equation (8b) becomes

$$\sum_j c_j [-\beta_j - a_1 \eta + p^2 \eta^2] S_j^a(\eta) = A \sum_j c_j S_j^a(\eta). \quad (11)$$

Multiplying from the left by $S_i^a(\eta)$ and integrating over the angular domain $[-1, 1]$, we obtain a generalised eigenvalues equation

$$\mathbf{M}\mathbf{c} = A\mathbf{B}\mathbf{c}. \quad (12)$$

The matrices involve the elements

$$[\mathcal{M}^k]_{ij} = \int_{-1}^1 S_i^a(\eta) \eta^k S_j^a(\eta) d\eta \quad (13)$$

which can be evaluated analytically using known properties of the Legendre polynomials [25]. Those of interest

here are given by

$$[\mathcal{M}^0]_{ij} = \frac{2}{2i+1} \frac{(i+m)!}{(i-m)!} \delta_{ij}, \quad (14a)$$

$$[\mathcal{M}^1]_{ij} = \frac{2}{2i+1} \frac{(i+m)!}{(i-m)!} \frac{1}{2j+1} [(j-m+1)\delta_{i,j+1} + (j+m)\delta_{i,j-1}], \quad (14b)$$

$$[\mathcal{M}^2]_{ij} = \frac{2}{2i+1} \frac{(i+m)!}{(i-m)!} \frac{1}{2j+1} \left[\frac{(j+1-m)(j+2-m)}{2j+3} \delta_{i,j+2} + \left(\frac{(j+1-m)(j+1+m)}{2j+3} + \frac{(j+m)(j-m)}{2j-1} \right) \delta_{i,j} + \frac{(j-1+m)(j+m)}{2j-1} \delta_{i,j-2} \right], \quad (14c)$$

and are calculated only once, at the first iteration. The elements of the matrices \mathbf{M} and \mathbf{B} are given by

$$[\mathbf{M}]_{ij} = -j(j+1) [\mathcal{M}^0]_{ij} - a_1 [\mathcal{M}^1]_{ij} + p^2 [\mathcal{M}^2]_{ij}, \quad (15a)$$

$$[\mathbf{B}]_{ij} = [\mathcal{M}^0]_{ij}. \quad (15b)$$

Assuming a given energy value p^2 , the angular part reduces to solving the generalised eigenvalues problem (12), i.e. finding the eigenvalue A (the separation constant) and the eigenvector \mathbf{c} (the coefficients of expansion (9)). At each iteration, the matrix \mathbf{M} is easily recalculated with the new energy value p .

2.1.2. Radial equation

Once the A eigenvalue is obtained from the angular equation, the scaled energy p^2 is to be found from solving the radial equation (8a). Setting $U(\xi) = (\xi^2 - 1)^{|m|/2} f(\xi)$ removes the singular term $m^2/(\xi^2 - 1)$ from the differential equation. A first boundary condition is

$$\lim_{\xi \rightarrow \infty} f(\xi) = e^{-p\xi}. \quad (16)$$

We can set a second boundary condition at the other end, when the electron is exactly in the centre of the molecular system ($\xi = 1$). We have to distinguish two cases. When $m = 0$

$$\lim_{\xi \rightarrow 1} f(\xi) = \xi^{-\frac{A}{2}} e^{\frac{p^2}{4}\xi^2 - \frac{a_2}{2}\xi}. \quad (17)$$

because the radial equation (8a) reduces to

$$\frac{df(\xi)}{d\xi} = \left(\frac{p^2}{2}\xi - \frac{a_2}{2} - \frac{A}{2\xi} \right) f(\xi). \quad (18)$$

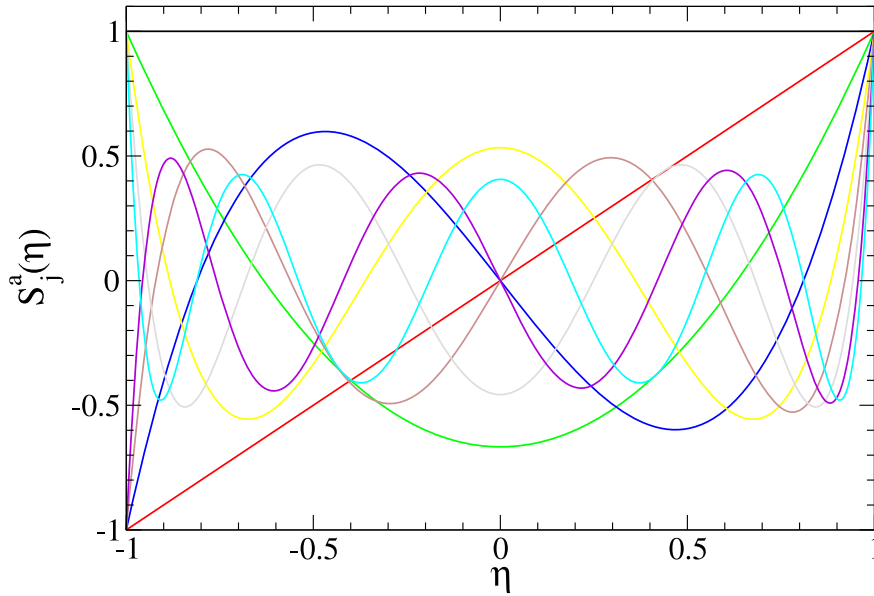


Figure 1. First 9 angular Sturmian basis elements $S_j^a(\eta)$ for $m = 0$.

For $m \neq 0$, the function $U(\xi)$ will vanish at $\xi = 1$ as long as $f(\xi)$ does not present any singularity at that value.

Similarly to the angular part, we propose an expansion

$$U(\xi) = (\xi^2 - 1)^{|m|/2} \sum_j d_j \mathcal{S}_j^r(\xi), \quad (19)$$

on a basis of Generalized Sturmian Functions $\mathcal{S}_j^r(\xi)$ generated by the Sturmian equation

$$\left[\frac{\partial}{\partial \xi} \left[(\xi^2 - 1) \frac{\partial}{\partial \xi} \right] + 2\xi |m| \frac{\partial}{\partial \xi} + a_2 \xi - p_s^2 \xi^2 \right] \mathcal{S}_j^r(\xi) = \alpha_j V_s(\xi) \mathcal{S}_j^r(\xi), \quad (20)$$

with eigenvalues α_j . In Equation (20), $p_s^2 = -\frac{R^2 E_s}{2}$ is a parameter that can be set freely. However, since the expansion over the GSF basis is meant to represent a physical radial function, it is convenient and numerically efficient to choose E_s according to the physics one wishes to describe. When dealing with a continuum state of energy $E > 0$, taking $E_s = E$ is a natural choice. In order to represent a specific bound state with an a priori unknown energy value, taking $E_s < 0$ close to a guess of the sought after energy turns out to be a good choice. In both continuum and bound cases, an appropriate choice of E_s will impose an adequate energy behaviour onto the GSF functions, ultimately making the basis more efficient from a convergence point of view. V_s , known as generating potential, must be a short range potential so that the basis elements $\mathcal{S}_j^r(\xi)$ have an asymptotic behaviour similar to (16), that is to say an exponential decay with energy E_s (taking E_s close to the correct sought after value E is then a natural choice). Moreover, since we wish $\mathcal{S}_j^r(\xi)$

to possess also the same $\xi \rightarrow 1$ behaviour as the sought after solution $U(\xi)$, the generating potential must obey the relation

$$\lim_{\xi \rightarrow 1} \alpha_j V_s(\xi) = -A + p^2 - p_s^2. \quad (21)$$

It turns out that it is convenient to choose a function nearly constant at $\xi = 1$, in order to stabilise the iterations. In the present work, the generating potential is chosen to be

$$V_s = \frac{1}{2} [1 - \tanh(\delta(\xi - \gamma))], \quad (22)$$

where the parameters δ and γ determine the shape of the potential as illustrated by Figure 2. For a given value of δ , a larger parameter γ extends the range of the potential (for $\delta = 1$, γ approximately represents the range). On the other hand, for a fixed value of γ (solid and dotted curves), higher δ parameters correspond to steeper potentials. As explained in the GSF references [15,16], the generating potential is crucial for the continuum functions. For bound type solutions, on the other hand, the choice of V_s is not so important (it does not affect noticeably the convergence of the method) but helps for example in regulating the radial domain covered by the GSF. We have not performed an exhaustive optimisation of the potential parameters, but we found, roughly, that changing these values by one order of magnitude affects the final bound state energy values only beyond the sixth significant figure. As a rule of thumb, our numerical investigation established that the values $\delta \approx 1$ and $\gamma \approx 5$ are a suitable choice for the potential parameters in the case of the ground state. For excited states with principal quantum number n , the potential range should be

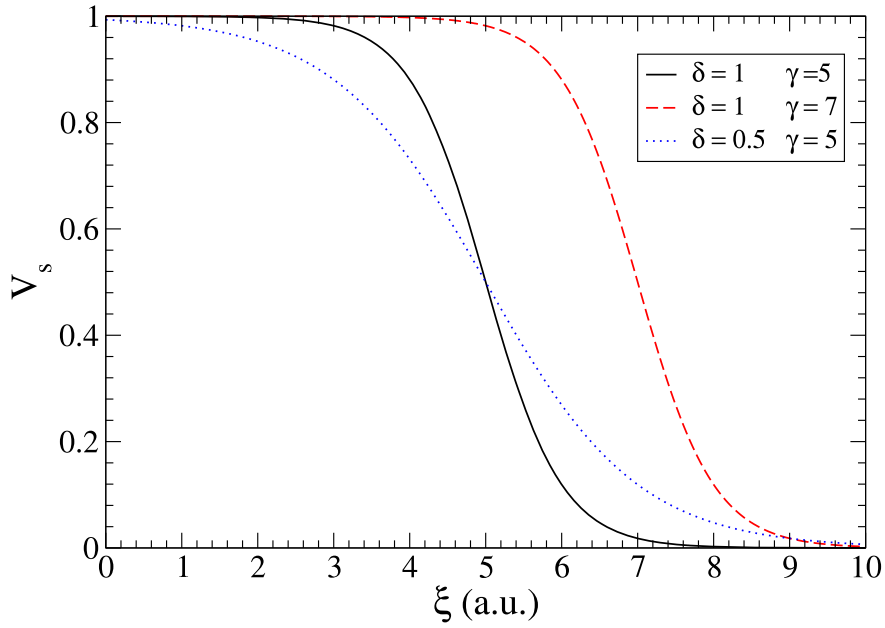


Figure 2. Generating potential V_s , used to generate the radial GSF $\mathcal{S}_j^r(\xi)$.

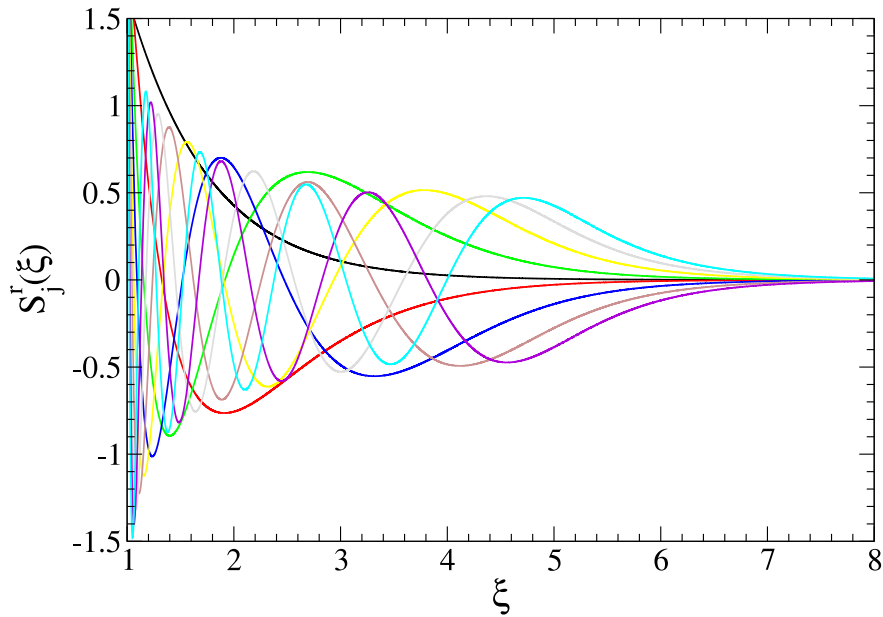


Figure 3. First 9 radial basis elements $\mathcal{S}_j^r(\xi)$ for $m = 0$.

incremented roughly by a factor $\frac{\Delta\gamma}{\Delta n} \approx 2$. Also, for varying internuclear distances R , it is convenient to scale the potential range by a factor $\frac{2}{R}$.

At $\xi \rightarrow \infty$ we could impose on $\mathcal{S}_j^r(\xi)$ the boundary condition (16), but requiring simply the basis function to vanish at infinity was found to be sufficient. On the other hand, imposing on each element condition (17) at $\xi \rightarrow 1$ results to be crucial when $m = 0$. We generate the Sturmian functions by solving the radial equation (20) with a finite difference method. In Ref [15] the reader can find a detailed description of the numerical procedures

used for the solution of the differential equation, which in turn, are based on the radial methods for the solution of the Schrödinger equation described in W. Johnson's book [26]. Briefly, the solution integration consists of a predictor-corrector Adams–Moulton method. It uses a seven-point scheme, which (together with the interpolation procedure) achieves a high order of accuracy (of about $(\Delta x)^8$). The original GSF code was developed primarily for Coulomb-type solutions and for high principal quantum numbers. Since these functions oscillate rapidly close to the nucleus and decay exponentially far away, one

may use a logarithmic grid generating a fine mesh near the origin and a coarse mesh for large distances. With this approach, very accurate results can be obtained by using only a few points (about 500) in the numerical grid. Since in the present investigation we are interested in the first eigenfunctions we can relax the numerical sophistication and complexity, and use a low-order Numerov approximation for the propagation, in a linear mesh. Of course, this replacement would require a large number of mesh points (about 10^4), but this is not a serious problem in a one-dimensional calculation. The numerical quadratures are evaluated using a trapezoidal rule with endpoint corrections developed by Johnson [26]. The first 9 basis elements for $m = 0$, generated with $\delta = 1.1$ and $\gamma = 5$, are shown in Figure 3. As j increases, these functions display an increasing number of nodes. Featuring one of the main GSF properties, all elements behave asymptotically in a unique manner, here in the same exponential manner $e^{-p_s \xi}$ as $\xi \rightarrow \infty$.

With expansion (19), and making use of (20), the radial equation (8a) takes the form

$$\begin{aligned} & \sum_j d_j [\alpha_j V_s(\xi) + A + m^2 + |m|] \mathcal{S}_j^r(\xi) \\ &= \sum_j d_j (p^2 - p_s^2) \xi^2 \mathcal{S}_j^r(\xi). \end{aligned} \quad (23)$$

Multiplying from the left by \mathcal{S}_i^r and integrating over the domain $[1, \infty[$, we obtain another generalised eigenvalue equation

$$\mathbf{N} \mathbf{d} = \lambda \mathbf{C} \mathbf{d} \quad (24)$$

where the eigenvalues are $\lambda = p^2 - p_s^2$, and thus the corresponding energies through $p^2 = -R^2 E/2$. Let us define the elements

$$[\mathcal{N}^k]_{ij} = \int_1^\infty \mathcal{S}_i^r(\xi) \xi^k \mathcal{S}_j^r(\xi) d\xi, \quad (25a)$$

$$[\mathbf{G}]_{ij} = \int_1^\infty \mathcal{S}_i^r(\xi) V_s(\xi) \mathcal{S}_j^r(\xi) d\xi, \quad (25b)$$

that are calculated, numerically, only once. The matrices \mathbf{N} and \mathbf{C} have for elements

$$[\mathbf{N}]_{ij} = (A + m^2 + |m|) [\mathcal{N}^0]_{ij} + \alpha_j [\mathbf{G}]_{ij}, \quad (26a)$$

$$[\mathbf{C}]_{ij} = [\mathcal{N}^2]_{ij}. \quad (26b)$$

Here, A is a fixed parameter obtained from the previous step, when solving the angular part. The solutions of (24) provide both the eigenvalues λ and the eigenvectors made of the coefficients d_j of the radial expansion (19).

This iterative method has a significant advantage. The Hamiltonian is separated into two coupled equations, and

both of them are one-dimensional reducing significantly the computational cost. Moreover, the use of expansions on GSF basis greatly simplifies the task since each basis element already solves a substantial part of the equations, in particular, the differential operators. As a consequence, it is not necessary to solve numerically the differential equations at each step. Computationally, one only solves – iteratively – two generalised eigenvalue problems. There is, however, a drawback in this methodology: each molecular state requires a new basis set. This means that, from all the eigenvalues A and p resulting from the calculations, we must select only those corresponding to the eigenvectors having the right number of nodes. For each one of the molecular states, a different iteration procedure is thus needed. This difficulty is avoided in the alternative method presented hereafter.

2.2. GSF: direct 2d method

We propose now a method in which equation (2) is solved directly. As before, we first remove the azimuthal part and write

$$\psi(\xi, \eta, \phi) = \Psi(\xi, \eta) \Phi(\phi) \quad (27)$$

with $\Psi(\xi, \eta)$ solution of the two-dimensional equation

$$\begin{aligned} & \left\{ \frac{\partial}{\partial \xi} \left[(\xi^2 - 1) \frac{\partial}{\partial \xi} \right] + a_2 \xi - p^2 \xi^2 - \frac{m^2}{\xi^2 - 1} \right. \\ & \left. + \frac{\partial}{\partial \eta} \left[(1 - \eta^2) \frac{\partial}{\partial \eta} \right] - a_1 \eta + p^2 \eta^2 - \frac{m^2}{1 - \eta^2} \right\} \\ & \Psi(\xi, \eta) = 0. \end{aligned} \quad (28)$$

This time we propose to expand the solution $\Psi(\xi, \eta)$ over a two-dimensional basis $S_{ij}(\xi, \eta)$

$$\begin{aligned} \psi(\xi, \eta) &= \sum_{ij} a_{ij} S_{ij}(\xi, \eta) \\ &= (\xi^2 - 1)^{|m|/2} \sum_{ij} a_{ij} \mathcal{S}_i^r(\xi) \mathcal{S}_j^a(\eta), \end{aligned} \quad (29)$$

where the one-dimensional Sturmian functions are obtained with the same methodology described above, i.e. from equations (10) and (20).

Upon substitution of expansion (29), the two-dimensional equation (28) becomes

$$\begin{aligned} & \sum_{ij} a_{ij} \left\{ \alpha_i V_s(\xi) + m^2 + |m| + p_s^2 \xi^2 - a_1 \eta - \beta_j \right\} \\ & S_{ij}(\xi, \eta) \\ &= \sum_{ij} a_{ij} p^2 (\xi^2 - \eta^2) S_{ij}(\xi, \eta). \end{aligned} \quad (30)$$

A matrix system is constructed by multiplying from the left by a basis element $S_{i'j'}(\xi, \eta)$ and integrating over both

ξ and η variables (note here the absence of the volume element $\xi^2 - \eta^2$ in spheroidal prolate coordinates). We obtain a generalised eigenvalues problem

$$\mathbf{P}\mathbf{a} = \lambda\mathbf{D}\mathbf{a}, \quad (31)$$

in which the matrices \mathbf{P} and \mathbf{D} are given by

$$\begin{aligned} [\mathbf{P}]_{i'j',ij} &= \alpha_i[\mathbf{G}]_{i'i'}[\mathcal{M}^0]_{jj} + p_s^2[\mathcal{N}^2]_{i'i}[\mathcal{M}^0]_{jj} \\ &\quad - a_1[\mathcal{N}^0]_{i'i}[\mathcal{M}^1]_{jj} + (m^2 + |m| - \beta_j) \\ &\quad [\mathcal{N}^0]_{i'i}[\mathcal{M}^0]_{jj}, \end{aligned} \quad (32a)$$

$$[\mathbf{D}]_{i'j',ij} = [\mathcal{N}^2]_{i'i}[\mathcal{M}^0]_{jj} - [\mathcal{N}^0]_{i'i}[\mathcal{M}^2]_{jj}. \quad (32b)$$

We solve this eigenvalue problem, obtaining a solution matrix \mathbf{a} ; each column consists of the coefficients vector \vec{a}^n , which expands that solution corresponding to the molecular state having eigenenergy $\lambda_n = p_n^2$. To be more specific, if the basis size is N , we have

$$\mathbf{a} = \begin{pmatrix} a_{11}^1 & a_{11}^2 & a_{11}^3 & \dots & a_{11}^N \\ a_{21}^1 & a_{21}^2 & a_{21}^3 & \dots & a_{21}^N \\ \dots & \dots & \dots & \dots & \dots \\ a_{12}^1 & a_{12}^2 & a_{12}^3 & \dots & a_{12}^N \\ a_{22}^1 & a_{22}^2 & a_{22}^3 & \dots & a_{22}^N \\ \dots & \dots & \dots & \dots & \dots \\ a_{ij}^1 & a_{ij}^2 & a_{ij}^3 & \dots & a_{ij}^N \\ \dots & \dots & \dots & \dots & \dots \end{pmatrix}, \quad \lambda = \begin{pmatrix} p_1^2 \\ p_2^2 \\ \dots \\ p_N^2 \end{pmatrix}. \quad (33)$$

This direct methodology avoids iterations. Moreover, it allows us to obtain the solutions for many molecular states simultaneously. Since the matrices are two-dimensional, at first sight the method seems computationally costly. However, all integrations leading to the matrix elements of \mathbf{P} and \mathbf{D} are separable and reduce to products of one-dimensional integrals as given by (32a) and (32b).

3. Results

We present now the results of our calculations and make a comparison with the data provided in the literature. We start by applying the GSF iterative 1d method for both the ground and some $m = 0$ excited states of the hydrogen molecular ion H_2^+ for which $Z_1 = Z_2 = 1$ and thus $a_1 = 0$. Next, we consider asymmetric (heteronuclear) molecular ions with $Z_1 \neq Z_2$. Finally, for H_2^+ , we will

Table 1. Convergence of the eigenvalue A in Equation (8b) for fixed energy $E = 1.10264$, as a function of the basis size.

Number of basis elements	A
1	0.7350895
2	0.8115139
3	0.8117295
4	0.8117296
Reference [27]	0.8117296

show how the GSF direct 2d method yields the ground and several excited states in a single run.

3.1. Iterative 1d method for the ground state of H_2^+

The best values of the energy E for the ground state $1\sigma_g$, and the corresponding separation constant A from the work of Scott *et al.* [27] are used here as a benchmark to analyse the convergence issues of our Sturmian method. We assume here an internuclear distance $R = 2$ a.u., thus fixing the values of a_1 and a_2 .

3.1.1. Angular equation

In order to solve the angular equation (8b), an initial value for the energy E (more precisely, $p^2 = 2.2052684$) is chosen. The matrices of the generalised eigenvalue problem (12) are easily constructed as they are all analytical. The only numerical aspect to analyse is the convergence of the results with respect to the basis size. Since the ground state is an even function in the ξ coordinate, only even elements $S_j^a(\eta)$ are included in the expansion. As shown through Table 1, convergence towards the benchmark result A of [27] is reached with just four elements.

Having solved the matrix equation, the eigenvectors give the coefficients c_j that allow us to construct the ground state angular solution (9) which is shown in Figure 4. The excited states will be discussed in the next section.

3.1.2. Radial equation

Once the angular equation is solved, we turn to the radial equation. In contrast to the angular part, here the approach is completely numerical. On the one hand, we have to generate the basis set $S_i^r(\xi)$ and, on the other, the matrix elements of the corresponding eigenvalue problem (24) must be calculated numerically.

The basis elements are generated by solving the Sturmian equation (20) with a numerical method described previously [15]. It is based on a predictor-corrector algorithm, propagating the solution from the origin to some defined matching point (this is the outgoing solution), and from an effective infinite towards this

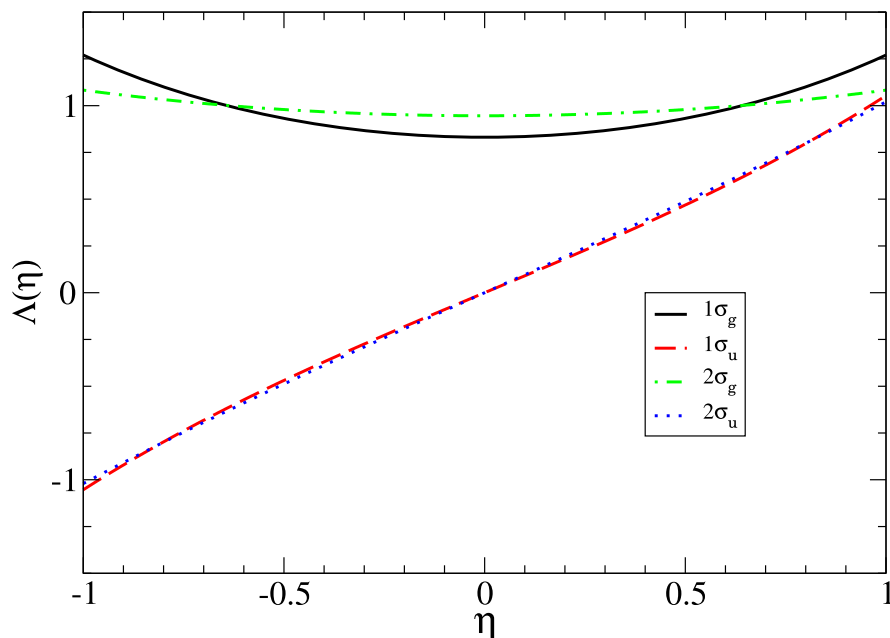


Figure 4. The angular $\Lambda(\eta)$ solutions for the four lower energy states of H_2^+ .

point (the inward solution). The inward function is normalised, in such a way that both solutions coincide at the matching point. If the derivatives disagree at this point, the eigenvalue is adjusted and the procedure starts again, until convergence. This algorithm, allows one to produce very accurate solutions for atomic systems, even with a reasonably small (~ 500) points in the numerical grid [15,16]. However, we noticed that it was hard to obtain the radial solutions of Equation (8a), even when a large number of points was included in the numerical grid. In fact, to solve this equation appropriately, the crucial aspect resides in the fulfillment of the boundary conditions (17) at the origin. We endorsed this conclusion, trying to solve the radial equation with other methods, and using different mathematical software, obtaining very different results for different numerical grids. We even tried to solve the equation fixing the energy value to $E = -1.10264$ a.u. [27], but the converged solutions yielded eigenvalues A too far from the correct value.

We also tried to use standard diagonalisation routines from LAPACK [28] to solve equation (8a) directly. However, within this approach, it is not simple to introduce explicitly the boundary conditions in contrast to our GSF expansion approach for which it is straightforward. Thus, our method allows us to obtain very accurate results, even with a very few numbers of points in the numerical grid. Nevertheless, since all the required integrals are one-dimensional, we used a significant number of points ($\sim 10^4$), regardless of whether it was necessary.

Table 2. Convergence of the energy E in Equation (8a) for fixed $A = 0.8117296$ as a function of the number of basis elements. The third column corresponds to the energy \tilde{E} obtained with an improved (recalculated) basis.

Basis elements	E (a.u.)	\tilde{E} (a.u.)
1	-1.0	-1.1
3	-1.1	-1.1026
6	-1.1024	-1.1026340
9	-1.1026	-1.1026346
Reference [6]	-1.1026342	

Having solved the Sturmian equation and generated the basis set $\mathcal{S}_i^r(\xi)$ for a chosen external parameter E_s , we can proceed to analyse convergence issues for the expansion (19) of the function $U(\xi)$. In Table 2, the basis size dependence of the energy value E , obtained by fixing the separation constant $A = 0.8117296$, is shown for two different sets. As explained in Section 2.1.2, the external parameter E_s is an arbitrary energy; however, it is convenient to choose a value close to the true state energy. In a first calculation, we took the value $E_s = -1$ a.u. and obtained the convergence sequence shown in the second column of Table 2 that leads to a state energy of $E = -1.1026$ a.u.. In a second, better, calculation we generate the radial GSF basis using as the external Sturmian energy, precisely this state energy, i.e., we set $E_s = -1.1026$ a.u.. In so doing, the sequence of energies obtained, listed in the third column of the table, converges very fast to the very accurate benchmark value.

Once the eigenvalues equation is solved, the eigenvectors of (24) provide the expansion coefficients d_i , which

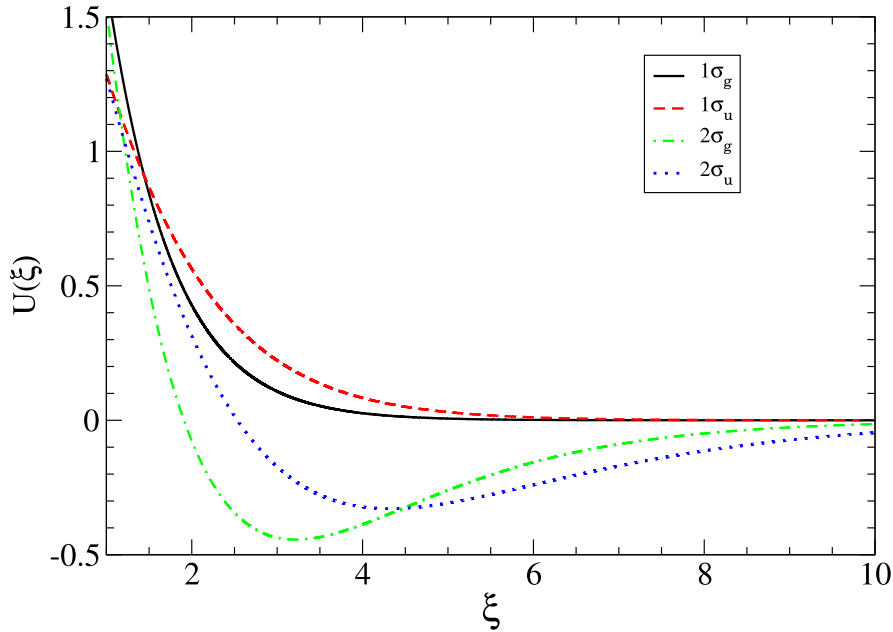


Figure 5. The radial $U(\xi)$ solutions for the four lower energy states of H_2^+ .

build the radial function $U(\xi)$ through (19). The converged result is shown in Figure 5; the excited states will be discussed in the next section.

The product of the angular and radial solutions $\Lambda(\eta)U(\xi)$ gives, up to the azimuthal dependence, the wavefunction which is best visualised by converting the prolates (ξ, η, ϕ) into Cartesian coordinates (x, y, z) through

$$x = \frac{R}{2} \sqrt{(1 - \eta^2)(\xi^2 - 1)} \cos(\phi), \quad (34a)$$

$$y = \frac{R}{2} \sqrt{(1 - \eta^2)(\xi^2 - 1)} \sin(\phi), \quad (34b)$$

$$z = \frac{R}{2} \eta \xi. \quad (34c)$$

In the top left panel of Figure 7, we show the obtained $\psi_{1\sigma_g}$ for a fixed angle ϕ (for $m = 0$ states, the results are symmetric respect to rotations over the z axis, and therefore, there is no dependence on the angle ϕ).

3.1.3. Internuclear distance dependence

In the ground state results presented above, we have fixed, adopting the Born–Oppenheimer approximation, the internuclear distance at $R = 2$ a.u. Calculations can be easily repeated by varying R , and in each case, one obtains the total energy

$$E_{\text{tot}}(R) = E(R) + \frac{1}{R}. \quad (35)$$

The radial Sturmian functions should be generated through Equation (20) in which one modifies $a_2 =$

$R(Z_1 + Z_2)$ for each R . This option can be taken but we found it convenient to use a unique basis generated with a given value $a_{2s} = R_s(Z_1 + Z_2)$; except for very high internuclear distances R , we simply took $R_s = 2$ a.u.. In so doing, the use of the Sturmian equation for the radial Schrödinger equation (8a) leads to a slightly modified Equation (23) and thus the supplementary matrix element $(a_2 - a_{2s})[\mathcal{N}^1]_{ij}$ must be added to matrix \mathbf{N} defined by (26a). We have calculated the total energy for many values of R taking 4 angular and 6 radial basis functions, generated with a Sturmian energy $E_s = -1.1026340$, which is the energy value obtained for $R = 2$ a.u. in the previous section. Figure 6 presents the resulting energy E_{tot} as a function of the internuclear distance. The inset allows one to see a clear minimum at $R = 1.99704$ a.u. At this equilibrium distance (bond length) the corresponding energy $E_{\text{tot}} = -0.602635$ a.u. is in agreement with the best values given in the literature [29].

We challenged our computational method with energy calculations considering very small internuclear distances R for which, in general, many numerical instabilities and errors arise. The energy values displayed in Table 3 demonstrate that our Sturmian method remains robust for decreasing distances R , even in the limit $R \rightarrow 0$, for which the solution corresponds to the atomic ion He^+ with energy $E_{\text{He}^+} = -Z^2/2 = -2$ a.u.. At the same time, the ground state wavefunction should evolve from a molecular to an atomic shape, that is to say from a density of probability centred on the two nuclei to a hydrogenic single centre system. This transition from molecular to

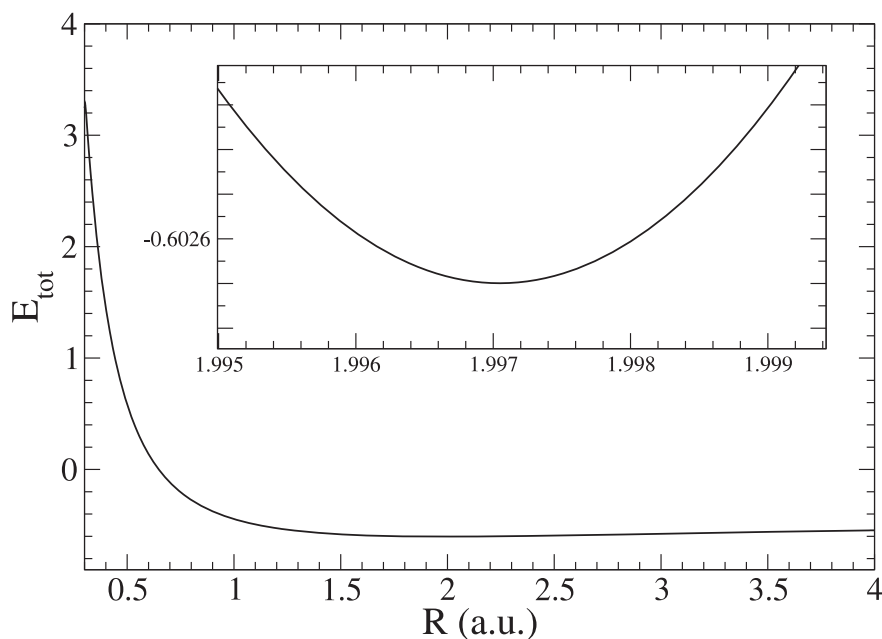


Figure 6. Total energy of the H_2^+ ground state as a function of the internuclear distance R .

Table 3. Ground state energy of the system $H + H + e^-$, as a function of the internuclear distance R .

R (a.u.)	E (a.u.)
2	-1.1026340
1	-1.4517823
0.4	-1.800754
0.1	-1.9782552
0.025	-1.9984113
0.008	-1.9998307
He^+	-2.0

the atomic system as the internuclear distance decreases is illustrated in Figure 7.

3.2. Iterative 1d method for some excited states of H_2^+

By modifying the way the GSF basis functions are constructed, the GSF spectral method allows one to obtain not only the ground state but also excited and continuum states. To start with, let us look at the first excited state $1\sigma_u$. For the generation of the radial basis, it is necessary to choose an arbitrary Sturmian energy as an external parameter. In a first, crude, approach we take the same energy obtained for the ground state calculation ($E_s = -1.10263$ a.u. or, equivalently, $p_s = 1.485015$). We generate then three Sturmians for the angular basis (only odd functions because of parity) and six radial Sturmian functions. With these functions, we carry out the iteration procedure, solving first the angular equation, obtaining the eigenvalue A . This value is introduced as a parameter into the radial equation, whose solutions produce a new scaled energy value p . As shown in Table 4, a

Table 4. Convergence of p and energy E for the first H_2^+ excited state $1\sigma_u$. The fifth column corresponds to the energy \tilde{E} obtained with an improved (recalculated) basis.

Iteration	p	E (a.u.)	\tilde{p}	\tilde{E} (a.u.)
0	1.485015	-1.10263	1.154791	-0.666771
2	1.175548	-0.690957	1.155444	-0.667525
4	1.155869	-0.668017	1.155451	-0.667534
6	1.154793	-0.666773		
8	1.154791	-0.666771		
Reference [27]	1.155452	-0.667534		

very precise result with six significant figures is obtained after only eight iteration steps. However, as we discussed for the ground state, we can make the whole calculation even better, choosing the Sturmian energy value from the last convergence step ($p_s = 1.154791$, or $E_s = -0.666771$ a.u.) and recalculating the radial basis. In so doing, the convergence is even faster, and only four iteration steps are sufficient to reach the energy values given by Scott [27].

The same procedure is repeated for the generation of other excited states, such as $2\sigma_g$ and $2\sigma_u$. In Table 5, the energy results obtained with our iterative method are displayed and compare very favourably with the results obtained by Bian [6]. Note that the latter coincide, up to the eighth decimal with those of Madsen and Peek [30].

The radial $U(\xi)$ and the angular $\Lambda(\eta)$ solutions of the four lowest states of H_2^+ are shown, respectively, in Figures 4 and 5. The total wavefunctions for the excited states $1\sigma_u$, $2\sigma_g$ and $2\sigma_u$ are shown in Figure 8 as a function of

the Cartesian coordinates (x, z) . We recall that the density is invariant under rotations around the z -axis.

3.3. Iterative 1d method for the asymmetric molecular ions HHe^{+2} and HLi^{+3}

We apply now our GSF approach to other mono-electronic diatomic systems, such as the HHe^{+2} and HLi^{+3}

molecular ions. For these heteronuclear ions, $Z_1 \neq Z_2$ and thus $a_1 \neq 0$. In order to compare with other sample results published in the literature, we have kept the internuclear distance fixed at $R = 4$ a.u. (for HHe^{+2} the equilibrium value is around $R = 3.89$ a.u.). These molecular ions are no longer symmetric along the $z = 0$ axis, so that the angular representation in Legendre polynomials requires many more elements than the $-$ symmetric $-\text{H}_2^+$

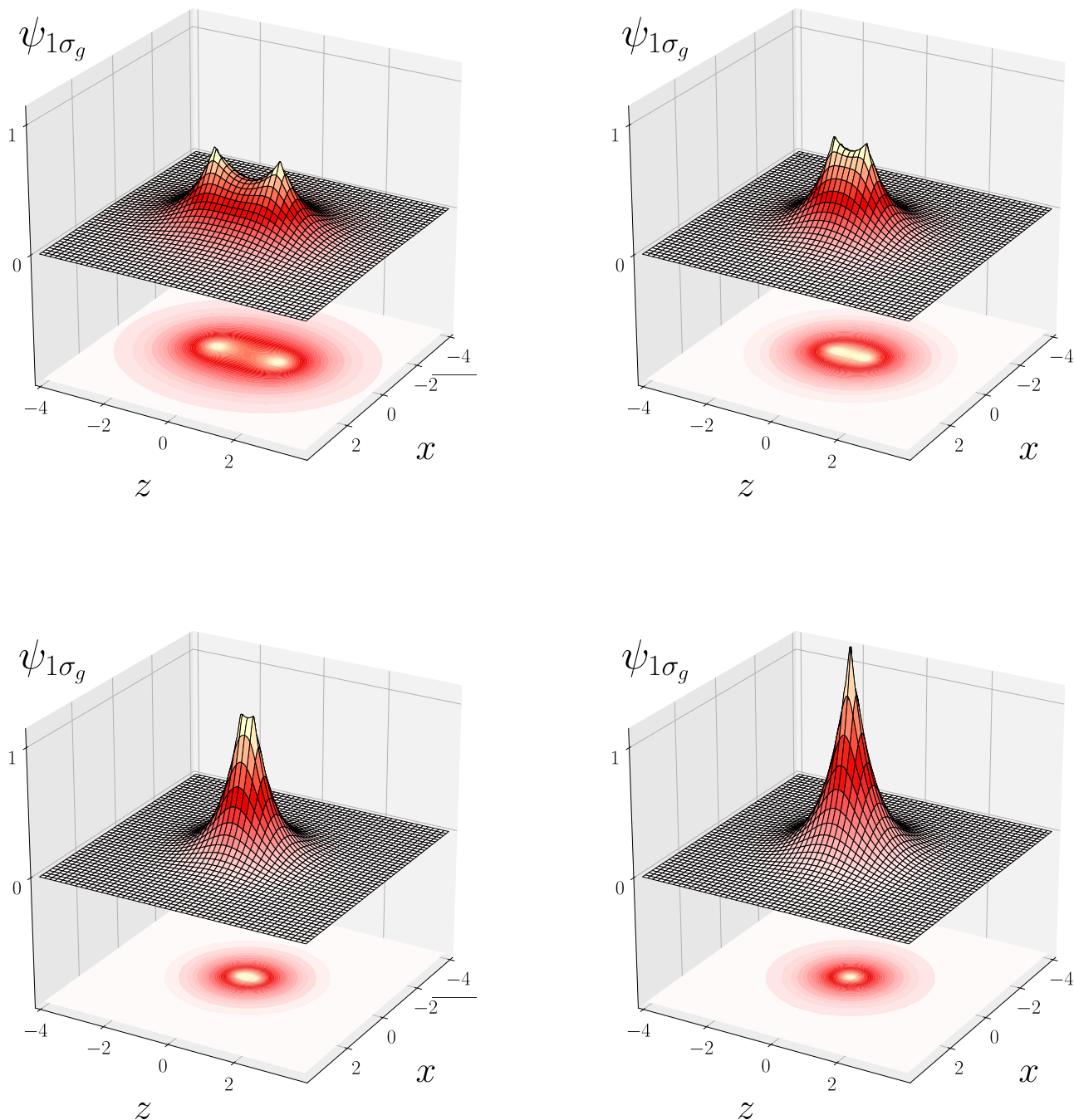


Figure 7. Wavefunction $\psi_{1\sigma_g}$ converted to cartesian coordinates, for the H_2^+ ground state, calculated at four different internuclear distances, moving from the molecular ion H_2^+ to the atomic ion He^+ : (top left) $R = 2.0$ a.u., (top right) $R = 1.0$ a.u., (bottom left) $R = 0.4$ a.u., (bottom right) $R = 0.008$ a.u. To better appreciate the evolution we have renormalised the wavefunctions.

Table 5. Parameter A and energies E of the lowest energy states of H_2^+ calculated with our iterative GSF method. The fourth column corresponds to the energy \bar{E} obtained with an improved (recalculated) basis. The last column reports the energy values found by Bian [6].

State	A	E (a.u.)	\bar{E} (a.u.)	E (a.u.) Ref. [6]
$1\sigma_g$	0.8117	-1.102	-1.1026340	-1.10263421
$1\sigma_u$	-1.8689	-0.667	-0.6675338	-0.66753439
$2\sigma_g$	0.2484	-0.3	-0.36081	-0.36086488
$2\sigma_u$	-1.69179	-0.25	-0.25535	-0.25541317

case. This said the computational cost is not significantly increased since all the angular integrals are analytical. For the HHe^{+2} molecular ion, we used 20 angular and 6 radial basis functions. We performed an initial calculation choosing the Sturmian energy $E_s = -3.0$ a.u., obtaining a ground state energy $E = -2.25060$, a value that was then recycled as the new E_s . For the HLi^{+3} molecular ion, we used 100 angular and 6 radial basis functions, starting with an initial guess $E_s = -5.0$ a.u., obtaining $E = -4.74968$ a.u. then recycled as the new E_s .

The ground state wavefunctions of the heteronuclear molecular ions are shown in Figure 9. The distribution of the electron density is now clearly asymmetric, the logical shift towards the nucleus with a larger charge being more evident as the Coulomb attraction increases. The shape of the wavefunction acquires more and more an atomic-like form centred on the heavier nucleus with only relatively small values close to the hydrogen nucleus. These features will obviously strongly depend on the internuclear distance, here fixed at $R = 4$ a.u..

Table 6 displays the calculated ground state energies, whose absolute value increases approximately as $Z_2^2/2$ with Z_2 the charge of the heavier nucleus. The efficiency of our method can be appreciated by giving a few numbers of other methods. The results given by Avery *et al.* [31] were calculated with 10 basis elements (Coulomb Sturmian functions) for each nucleus. Kereselidze *et al.* [32] used 10 basis functions per nucleus (Coulomb Sturmian in prolate spheroidal coordinates). Xue-Bin Bian [6] employed an imaginary-time-propagation method based on a Crank-Nicolson scheme to solve the separate equations, using 20 B-splines of order 7 to solve the radial equation, and 80 B-splines of order 7 for the angular part. Campos *et al.* [33] used 22 functions per coordinate. The aim of our calculation here was not to obtain very high accuracies, but rather to demonstrate that our simple and versatile method is computationally more efficient when compared to other approaches. If desired, we can achieve even better energy accuracies

Table 6. Ground state energies for the mono-electronic molecular ions: H_2^+ , assuming an internuclear distance $R = 2$ a.u., and HHe^{+2} and HLi^{+3} , assuming an internuclear distance $R = 4$ a.u.

	$E_{1\sigma_g\text{H}_2^+}$ (a.u.)	$E_{1\sigma\text{HHe}^{+2}}$ (a.u.)	$E_{1\sigma\text{HLi}^{+3}}$ (a.u.)
This work	-1.1026340	-2.2506056	-4.7501126
Avery [31]	-1.10220	-	-4.75011
Kereselidze [32]	-1.102614	-	-4.750111
Bian [6]	-1.1026342	-2.2506054	-
Campos [33]	-	-2.2506054	-4.7501118

by improving the employed numerical methods (number of points or the finite differences order) or by tuning the generating potential as to optimise the GSF basis set.

4. Direct $2d$ method for the ground and excited states of H_2^+

Although we found excellent results with the iterative method, we wish to exploit the full advantages of the spectral method, which allows one to obtain many states in one shot. The direct diagonalisation of a $2d$ Hamiltonian is generally very costly from the computational point of view. Within the finite differences framework, and taking into account that every coordinate has to be represented by hundreds of points, the matrix becomes huge and is intractable. A spectral method can reduce significantly the size of the Hamiltonian matrix to diagonalise, but computationally it still represents a hard task. Within the GSF method, the size of the matrices are reduced even more, since the appropriate physical behaviour is explicitly introduced in the basis set. In this manner, the numerical treatment is optimised.

The use of expansion (29) on a two-dimensional basis $S_{ij}(\xi, \eta)$ transforms the Schrödinger equation into an equation (30) where all the derivatives have been removed and replaced by simple expressions. Moreover, since the basis functions are optimised, the size of the basis is very small. For example, in our calculations, we introduced only 18 functions (3 angular $S_j^a(\eta)$ and 6 radial $S_i^r(\xi)$). Finally, the direct diagonalisation of this small matrix produces, as a result, 18 states simultaneously without the need to perform separate iterations for each state.

We have applied our GSF direct $2d$ method to the benchmark ion H_2^+ , again taking $R = 2$ a.u.. With only one diagonalisation we obtained the energy values displayed in Table 7. They compare very well with the results of Madsen and Peek [30], following their states notation. We should point out that our aim here was to produce all the levels at the same time without a focus on a single state. To generate the Sturmian basis, we chose here the energy value $E_s = -0.2$ a.u. which is clearly quite different from the ground state energy; it is an acceptable

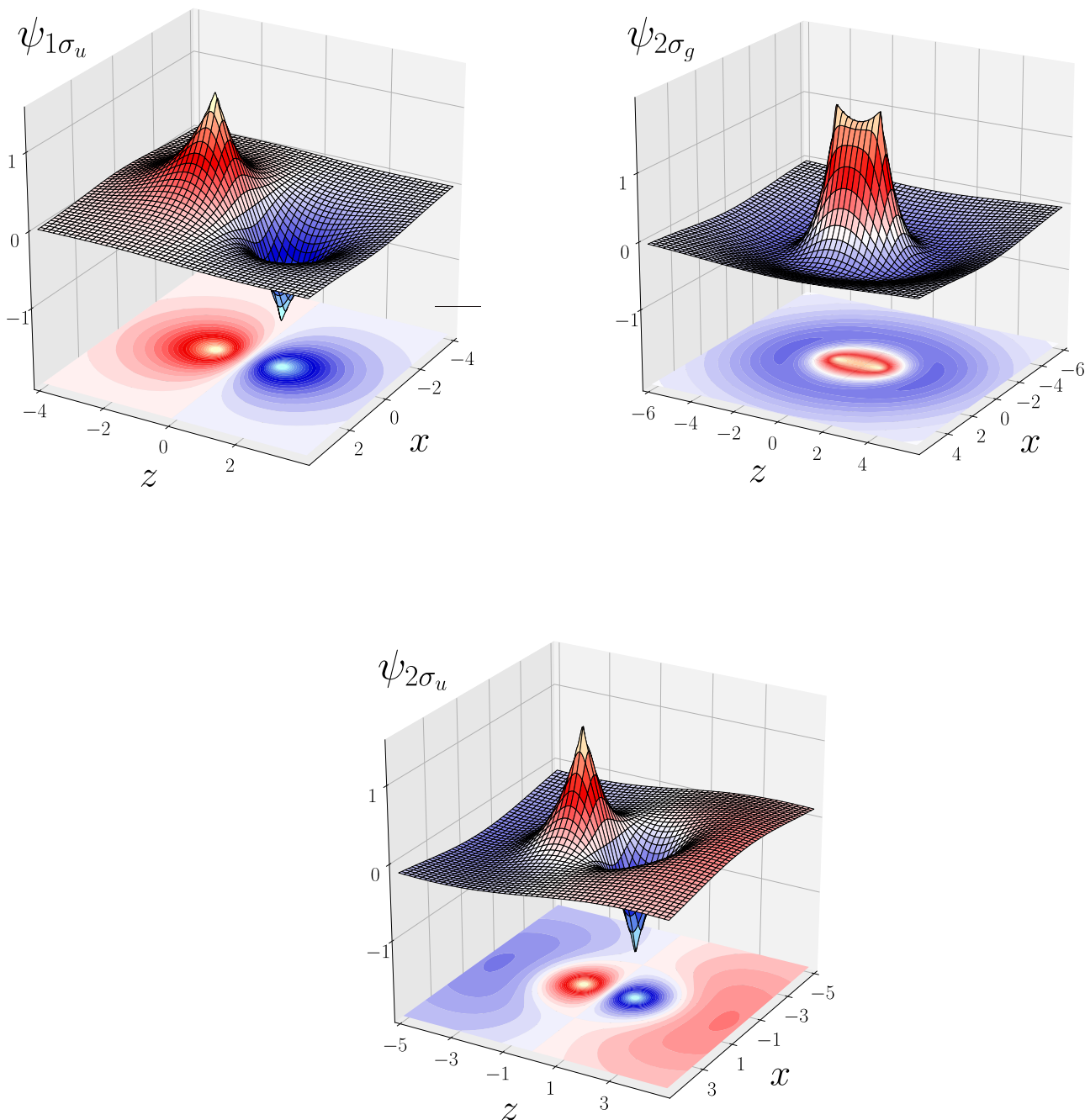


Figure 8. Wavefunctions for the first excited states $1\sigma_u$, $2\sigma_g$ and $2\sigma_u$ of H_2^+ .

Table 7. Energies of seven energy states of H_2^+ , obtained with the GSF direct $2d$ method. The third column indicates the results of Madsen and Peek [30]. Both were obtained for a fixed internuclear distance $R = 2$ a.u.

State	E (a.u.)	E (a.u.) Ref. [30]
$1\sigma_g$	-1.102630	-1.10263421
$2P\sigma_u$	-0.66753431	-0.66753439
$2S\sigma_g$	-0.360863	-0.36086488
$3P\sigma_u$	-0.25541312	-0.25541317
$3D\sigma_g$	-0.2357775	-0.23577763
$3S\sigma_g$	-0.1776	-0.17768105
$4P\sigma_u$	-0.133	-0.13731293

compromise that leads to a good precision for the whole set of presented molecular states. The table shows that it is possible to obtain excellent results, in particular for the lower states, at a rather small computational cost. If one wishes to improve the energy accuracy for one particular state, a different Sturmian energy E_s closer to this state energy should be chosen, as was shown in the $1d$ method. Since the generation of a new Sturmian basis requires one-dimensional calculations and the $2d$ matrix only has a few dozen elements, this further optimisation procedure is rather inexpensive.

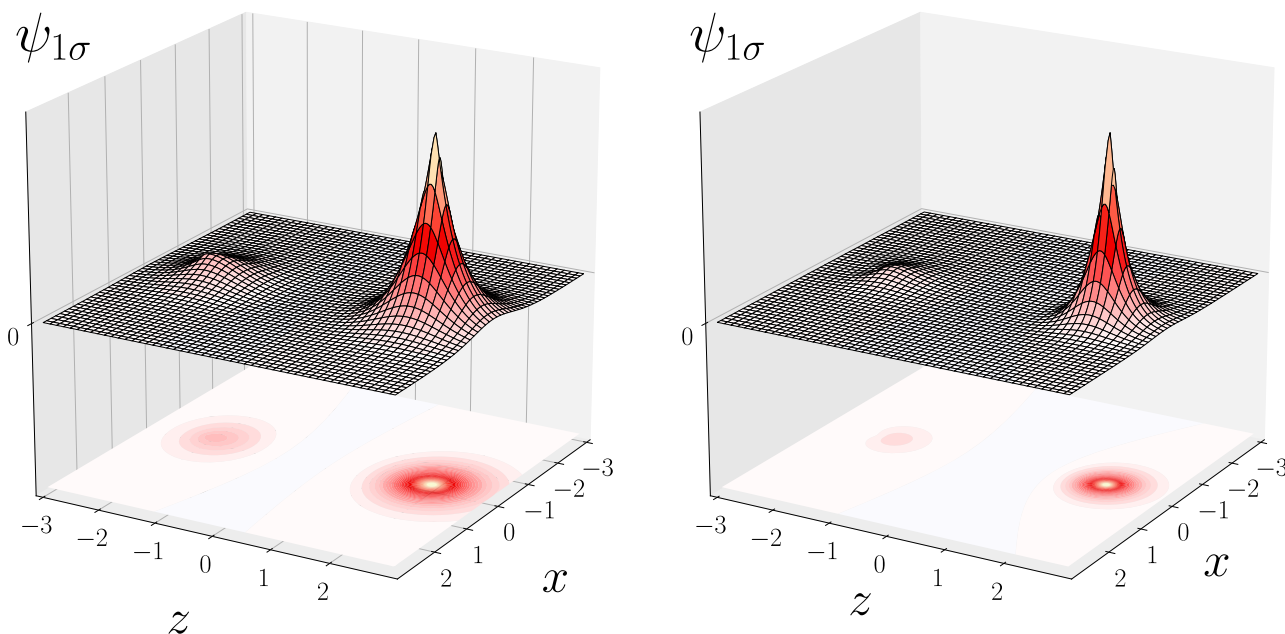


Figure 9. Unnormalised ground state wavefunctions 1σ of HHe^{+2} (left) and HLi^{+3} (right), assuming an internuclear distance $R = 4$ a.u..

5. Conclusion

The spectral method, based on Generalized Sturmian Functions, has been here extended, to allow its use in prolate spheroidal coordinates which should provide, in principle, the most effective framework to treat diatomic molecular systems. We developed and implemented two different numerical methods for the calculation of the molecular structure of mono-electronic molecular ions.

The first one consists in separating the Schrödinger equation in one angular and one radial equations, coupled through the energy and a coupling parameter. The equations are solved alternately, fixing the energy and the coupling parameter in each case, and after a few iterations, these parameters converged to the final values. The advantage of using GSF is twofold. On the one hand, it allows one the replacement of most of the Hamiltonian calculations by a simple expression thus substantially reducing the complexity of the calculation at any iteration step. On the other hand, the GSF method is based on the valuable property that the right boundary conditions are enforced onto the basis functions. Therefore, the size of the basis is minimal, turning the method in a very efficient procedure that produces ground and excited states of high quality.

The second method also uses GSF, and the angular and radial basis sets are generated in the same way as in the first one. Then, a two-dimensional basis set is constructed, and the Schrödinger equation solution becomes a $2d$ generalised eigenvalues problem. Since the basis

elements have the correct boundary conditions, the size of the basis is very small, and the diagonalisation is not a costly procedure. This direct $2d$ method does not require any iteration and a single calculation yields – simultaneously – many molecular states. Very good results can be obtained already with small basis set size. Both methods are computational efficient, but a quantitative comparison is not appropriate. Indeed, in the $1d$ iterative method, the GSF basis is generated as to focus on one particular state and great accuracy can be achieved. In contrast, the direct $2d$ method uses the same GSF basis to obtain a set of orthogonal bound states, and thus provides richer results albeit of relatively inferior accuracy. Besides, the spectrum obtained by diagonalisation may include discretised states of the continuum which can be useful for collision studies. In other words, one may state that the $1d$ iteration method is optimal to focus on a specific state while the $2d$ method provides a global view of the spectrum.

As a first step towards the extension of the GSF method to diatomic molecules, we have presented here an investigation of molecular ions having only one electron. We calculated the ground and excited states of the molecular hydrogen ion H_2^+ , in excellent agreement with benchmark results (7 significant figures in the case of the ground state). We also studied heteronuclear molecular ions, like HHe^{+2} and HLi^{+3} , with again excellent results. The method proved to be robust over a wide range of internuclear distances R , including in the notoriously difficult atomic limit.

The whole numerical investigation gives us confidence in our implementation of the GSF method in prolate spheroidal coordinates, as to contemplate exploring the continuous part of the spectrum. As demonstrated for atomic systems, the advantages of the GSF spectral method are more evident in the treatment of collision problems. In this case, the continuum Sturmian basis elements are generated with a positive energy parameter E_s and one imposes appropriate scattering boundary conditions. As a consequence, the basis needs to solve the Schrödinger equation only in the interaction region. Scattering problems involving one or two electrons in the continuum can then be treated efficiently with compact bases [16,18–20]. The same arguments apply to diatomic molecular systems, and we plan to extend the present investigation in prolate spheroidal coordinates to scattering problems such as single or double ionisation by photon or electron impact. First, we will examine the single continuum by studying the single photoionisation of the benchmark one-electron molecular ion H_2^+ ; then, we will move to the more challenging two-electron correlated case, by investigating single and double ionisation processes on H_2 and on quasi two-electron targets like N_2 as done for example in [34,35].

Disclosure statement

No potential conflict of interest was reported by the author(s).

Funding

D.M.M. gratefully acknowledge the financial support from the following Argentine institutions: Consejo Nacional de Investigaciones Científicas y Técnicas (CONICET), PIP 11220130100 607, Agencia Nacional de Promoción Científica y Tecnológica (ANPCyT) PICT-2017-2945, and Universidad de Buenos Aires UBACyT 20020170100727BA.

References

- [1] Ø. Burrau, Kgl. Danske, Videnskab. Selskab. Mat. Fys. Medd. 7, 14 (1927).
- [2] E.A. Hylleraas, Z. Phys. 71, 739–763 (1931). doi:10.1007/BF01344443
- [3] G. Jaffé, Z. Phys. 87, 535–544 (1934). doi:10.1007/BF0133263
- [4] B.H. Bransden and C.J. Joachain, *The Physics of Atoms and Molecules* (Longman Scientific and Technical, Harlow, UK, 1983).
- [5] A. Carrington, I.R. McNab and C.A. Montgomery, J. Phys. B 22, 3551 (1989). doi:10.1088/0953-4075/22/22/006
- [6] X.B. Bian, Phys. Rev. A 90, 033403 (2014). doi:10.1103/PhysRevA.90.033403
- [7] T. Kereselidze, I. Irakli Noselidze and A. Devdariani, J. Phys. B: At. Mol. Opt. Phys. 52, 105003 (2019). doi:10.1088/1361-6455/ab181e
- [8] V.V. Serov, B.B. Joulakian, D.V. Pavlov, I.V. Puzynin and S.I. Vinitzky, Phys. Rev. A 65, 062708 (2002). doi:10.1103/PhysRevA.65.062708
- [9] O. Chuluunbaatar, B.B. Joulakian, K. Tsookhuu and S.I. Vinitzky, J. Phys. B: At. Mol. Opt. Phys. 37, 2607 (2004). doi:10.1088/0953-4075/37/12/015
- [10] V.V. Serov, B.B. Joulakian, V.L. Derbov and S.I. Vinitzky, J. Phys. B: At. Mol. Opt. Phys. 38, 2765 (2005). doi:10.1088/0953-4075/38/15/014
- [11] O. Chuluunbaatar, B.B. Joulakian, I.V. Puzynin, Kh. Tsookhuu and S.I. Vinitzky, J. Phys. B: At. Mol. Opt. Phys. 41, 015204 (2008). doi:10.1088/0953-4075/41/1/015204
- [12] L. Tao, C.W. McCurdy and T.N. Rescigno, Phys. Rev. A 79, 012719 (2009). doi:10.1103/PhysRevA.79.012719
- [13] V.V. Serov and B.B. Joulakian, Phys. Rev. A 80, 062713 (2009). doi:10.1103/PhysRevA.80.062713
- [14] M. Foster, J. Colgan, O. Al-Hagan, J.L. Peacher, D.H. Madison and M.S. Pindzola, Phys. Rev. A 75, 062707 (2007). doi:10.1103/PhysRevA.75.062707
- [15] D.M. Mitnik, F.D. Colavecchia, G. Gasaneo and J.M. Randazzo, Comp. Phys. Comm. 182, 1145 (2011). doi:10.1016/j.cpc.2011.01.016
- [16] G. Gasaneo, L.U. Ancarani, D.M. Mitnik, J.M. Randazzo, A.L. Frapiccini and F.D. Colavecchia, Adv. Quantum Chem. 67, 153–216 (2013). doi:10.1016/B978-0-12-411544-6.00007-8
- [17] J.M. Randazzo, L.U. Ancarani, G. Gasaneo, A.L. Frapiccini and F.D. Colavecchia, Phys. Rev. A 81, 042520 (2010). doi:10.1103/PhysRevA.81.042520
- [18] J.M. Randazzo, D. Mitnik, G. Gasaneo, L.U. Ancarani and F.D. Colavecchia, Eur. Phys. J. D 69, 189 (2015). doi:10.1140/epjd/e2015-60113-9
- [19] M.J. Ambrosio, D.M. Mitnik, A. Dorn, L.U. Ancarani and G. Gasaneo, Phys. Rev. A 93, 032705 (2016). doi:10.1103/PhysRevA.93.032705
- [20] M.J. Ambrosio, L.U. Ancarani, A.I. Gomez, E.L. Gaggioli, D.M. Mitnik and G. Gasaneo, Eur. Phys. J. D 71, 127 (2017). doi:10.1140/epjd/e2017-70713-x
- [21] C. Granados-Castro, Ph. D. thesis, Université de Lorraine, 2016.
- [22] C.M. Granados-Castro, L.U. Ancarani, G. Gasaneo and D.M. Mitnik, Adv. Quantum Chem. 73, 3 (2016). doi:10.1016/bs.aiq.2015.06.002
- [23] C.M. Granados-Castro and L.U. Ancarani, Eur. Phys. J. D 71, 65 (2017). doi:10.1140/epjd/e2017-70721-x
- [24] E. Ali, C. Granados, A. Sakaamini, M. Harvey, L.U. Ancarani, A.J. Murray, M. Dogan and D. Madison, J. Chem. Phys. 150, 194302 (2019). doi:10.1063/1.5097670
- [25] A.R. Edmonds, *Angular Momentum in Quantum Mechanics* (Princeton University Press, Princeton, NJ, 1957).
- [26] W.R. Johnson, *Atomic Structure Theory* (Springer-Verlag Berlin Heidelberg, 2007).
- [27] T.C. Scott, M. Aubert-Frécon and J. Grotendorst, Chem. Phys. 324, 323 (2006). doi:10.1016/j.chemphys.2005.10.031
- [28] Linear Algebra PACKage, preprint (2017). <http://www.netlib.org/lapack/>.

- [29] L.J. Schaad and W.V. Hicks, *J. Chem. Phys.* 53, 851 (1970). doi:[10.1063/1.1674078](https://doi.org/10.1063/1.1674078)
- [30] M.M. Madsen and J.M. Peek, *At. Data Nucl. Data Tables* 2, 171 (1971).
- [31] J. Avery and J. Avery, *J. Phys. Chem. A* 113, 14565 (2009). doi:[10.1021/jp9040502](https://doi.org/10.1021/jp9040502)
- [32] T. Kereselidze, G. Chkadua and P. DeFrance, *Mol. Phys.* 113, 3471–3479 (2015). doi:[10.1080/00268976.2015.1036146](https://doi.org/10.1080/00268976.2015.1036146)
- [33] J.A. Campos, D.L. Nascimento, D.T. Cavalcante, A.L.A. Fonseca and A.O.C. Nunes, *Int. J. Quantum Chem.* 106, 2587 (2006). doi:[10.1002/\(ISSN\)1097-461X](https://doi.org/10.1002/(ISSN)1097-461X)
- [34] O. Chuluunbaatar, A.A. Gusev and B.B. Joulakian, *J. Phys. B: At. Mol. Opt. Phys.* 45, 015205 (2012). doi:[10.1088/0953-4075/45/1/015205](https://doi.org/10.1088/0953-4075/45/1/015205)
- [35] A.A. Bulychev and B. Joulakian, *J. Phys. B: At. Mol. Opt. Phys.* 46, 185203 (2013). doi:[10.1088/0953-4075/46/18/185203](https://doi.org/10.1088/0953-4075/46/18/185203)